Density Functional Study toward Understanding Dehydrogenation of the Adenine−Thymine Base Pair and Its Anion

Hujun Xie, Fei Xia, and Zexing Cao*

Department of Chemistry and State Key Laboratory of Physical Chemistry of Solid Surfaces, Xiamen University, Xiamen 361005, China

Received: December 15, 2006; In Final Form: March 11, 2007

The dehydrogenated radicals and anions of Watson−Crick adenine−thymine (A−T) base pair have been investigated by the B3LYP/DZP++ approach. Calculations show that the dehydrogenated radicals and anions have relatively high stabilities compared with the single base adenine and thymine. The electron attachment to the A−T base pair and its derivatives significantly modifies the hydrogen bond interactions and results in remarkable structural changes. As for the dehydrogenated A−T radicals, they have relatively high electron affinities and different dehydrogenation properties with respect to their constituent elements. The relatively low-cost hydrogen eliminations correspond to the (N9)−H (adenine) and (N1)−H (thymine) bonds cleavage. Both dehydrogenation processes have Gibbs free energies of reaction $\Delta G°$ of 13.4 and 17.2 kcal mol^{-1}, respectively. The solvent water exhibits significant effect on electron attachment and dehydrogenation properties of the A−T base pair and its derivatives. In the dehydrogenating process, the anionic A−T fragment gradually changes its electronic configuration from π^* to σ^* state, like the single bases adenine and thymine.

1. Introduction

In recent years, there has been increasing interest in the damage of DNA. The damage may cause the DNA mutation, resulting in various diseases such as the cancer.[1−5] Many experimental and theoretical efforts have been directed to DNA cleavage, and possible consequences and mechanisms of DNA damage and corresponding structural changes of the base pairs have been well studied, but still there are processes that are not well understood. Generally, the DNA damage may arise from radiations,[6−11] low-energy electron attachment,[12−17] and chemical reactions.[18−20] These damage ways are interrelated and interact on each other, which makes the damage mechanism more complicated.

As the constituent elements of DNA, the purine and pyrimidine bases have attracted considerable attention,[21−27] both experimentally and theoretically. Previous studies show that the presence of excess electron in the bases significantly modifies their properties such as fragmentation, structure, transfer of genetic information, etc. Electron attachment to the DNA base was assumed to be a crucial step for radiation damage of DNA, and much research has been carried out to elucidate mechanistic details.

Early experiments indicate that the nonthermal secondary electrons (3−20 eV) may efficiently induce single and double strand breaks, and such DNA damage takes place through transient negative ion states localized on the basic components of the DNA plasmid.[28−31] Recent experimental observations[32−34] show that the molecular anions of uracil, thymine, and adenine in the gas phase can be produced through Rydberg electron attachment due to the existence of dipole-bound parent anions. Further experiments by Mark and co-workers[35] found that the major dehydrogenated anions can be generated in electron attachment to DNA bases, but the site of the hydrogen abstraction has not been resolved.

Theoretical studies suggest that the nitrogen site is generally more favorable than the carbon site for the deprotonation process in pyrimidine bases.[36−37] Our recent calculations on purine bases also lend support to this conclusion.[38] Experimental studies on nucleosides show that the loss of a neutral hydrogen atom is from the anionic 2′-deoxyribothymidine[39−40] and low-energy electrons can efficiently break the N1−glycosidic bond.[41−43] Calculations on nucleosides have determined the adiabatic electron affinities (AEA) of stable nucleosides,[44] as well as the structure and relative energetics of the H-deleted radicals and anions in adenosine.[45] The AEA values of nucleosides are in the range from 0.99 to 3.47 eV, slightly larger than that of the single DNA base.

Computational study of the excess charge in DNA has been extended to the Watson−Crick base pairs in the gas-phase recently. Using the B3LYP/DZP++ method elaborated for DNA bases, Schaefer[46−47] and co-workers predict that the AEA values of the A−T and C−G base pairs are 0.36 and 0.60 eV, respectively, which are comparable with B3LYP/6-31+G(d) and SCC−DFTB−D results.[48−49] Their calculations[50−51] also determined the structure and energetics of the dehydrogenated C−G radicals and anions. Theoretical calculations[52−55] on the one-electron reduced or oxidized base pairs have been performed. The results show that these redox processes modify the strength of hydrogen bond and the pairing ability and cause proton transfer along hydrogen bond.

Although fragmentations of the single DNA bases A and T have been extensively investigated theoretically, no theoretical study of hydrogen loss in A−T base pair has been performed. Experimentally, the direct experimental measurement of AEA is quite difficult for the dehydrogenated A−T base pair, and complemented theoretical calculations may provide important information for determination of these qualities. Here, we

* Corresponding author. Fax: +86-592-2183047. E-mail: zxcao@xmu.edu.cn.

10.1021/jp0686137 CCC: $37.00
Published on Web 05/03/2007

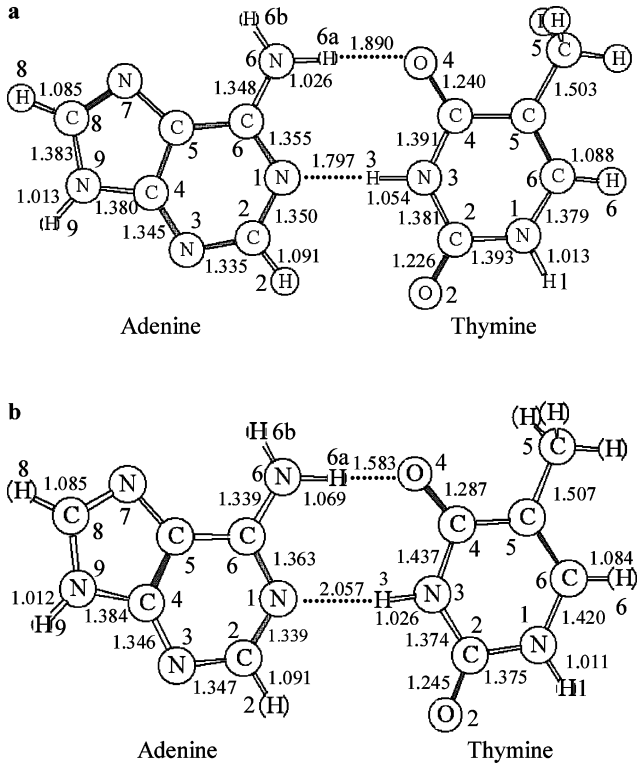

Figure 1. Optimized geometries and atomic numberings of the A−T base pair (a) and its anion (b).

performed a comprehensive study of the dehydrogenated A−T base pair by the density function approach and the effect of electron attachment to the A−T base pair on dehydrogenation has been discussed.

2. Computational Details

The geometries of the A−T base pair radicals and their respective anionic derivatives have been optimized by the B3LYP functional[56−57] with the DZP++ basis set[58] elaborated for the DNA base. Vibrational frequency analyses have been employed to assess the nature of optimized structures. The basis set superposition error (BSSE) correction was estimated by the Boys−Bernardi counterpoise method.[59,60] The natural population analysis (NPA) charges have been determined according to the natural bond order (NBO) analysis proposed by Reed and Weinhold colleagues.[61−64] A series of constrained optimizations along the C−H or N−H bond dissociation were performed in the potential energy surface (PES) scan.

To examine solvent effect on electron affinities and dehydrogenation properties, the CPCM polarizable conductor model[65−66] implemented in Gaussian 03 package[67] has been employed in geometry optimization and frequency analysis.

Test calculations on A−T pair show that predicted hydrogen-bond lengths at the B3LYP/DZP++ level of theory are in good agreement with available theoretical[68−73] and experimental values.[74] For example, the optimized N6−O4 and N1−N3 distances of A−T pair (Figure 1) are 2.91 and 2.85 Å, respectively, which match the experimental values of 2.95 and 2.82 Å very well.[74]

The adiabatic electron affinity (AEA) is determined as the energy difference between the appropriate neutral and anion at their respective optimized geometries:

$$\mathrm{AEA} = E_{(\text{optimized neutral})} - E_{(\text{optimized anion})}$$

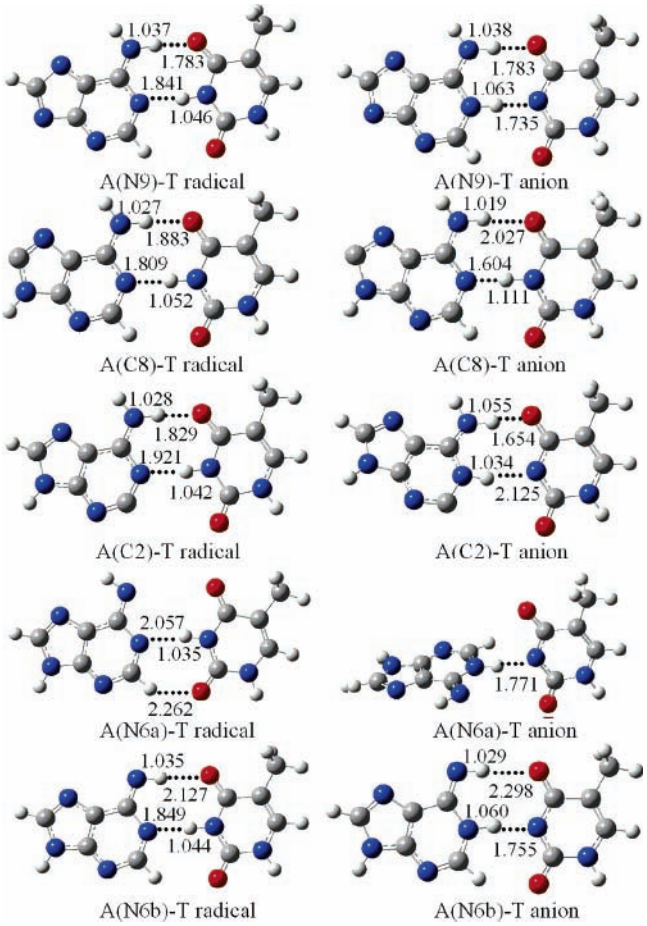

Figure 2. Optimized geometries of the adenine-dehydrogenated A−T radicals and anions.

The vertical electron affinity (VEA) is defined as the energy difference between the neutral species and the anion species at the optimized neutral geometry:

$$\mathrm{VEA} = E_{(\text{optimized neutral})} - E_{(\text{anion at the optimized neutral geometry})}$$

The vertical detachment energies (VDE) are computed as the energy difference between the neutral species and the anion species, both at the optimized anion geometry:

$$\mathrm{VDE} = E_{(\text{neutral at optimized anion geometry})} - E_{(\text{optimized anion})}$$

3. Results and Discussion

Optimized geometries and atomic numberings of the A−T base pair and its anion are presented in Figure 1. Figures 2 and 3 display optimized structures of dehydrogenated neutral radicals and their corresponding anions from the A−T pair. The dehydrogenating sites in A−T base pair radicals and anionic counterparts are indicated by the atom with numbering in parentheses. The dehydrogenated fragments are labeled according to the site of hydrogen-deleted atom in the parent base pair. For example, fragment notations **A(N6a)−T** and **A−T(C5)** denote structures from the hydrogen loss at the N6a site in adenine and at the C5 site in thymine, respectively.

Relative energies, natural charge populations, electron affinities, thermodynamic values, and dissociation energies for the A−T base pair derivatives are collected in Tables 1−5. Predicted potential energy surface profiles along different dehydrogenation channels are depicted in Figure 4.

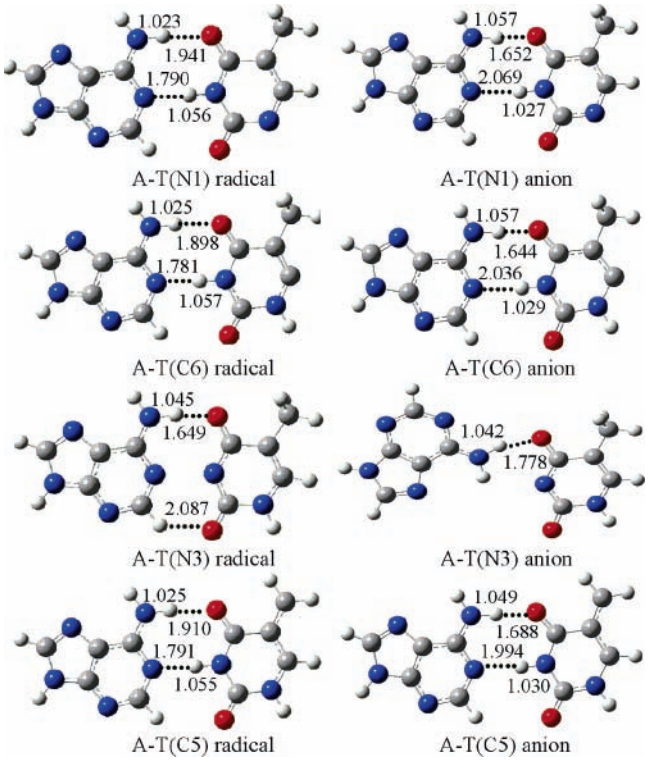

Figure 3. Optimized geometries of the thymine-dehydrogenated A−T radicals and anions.

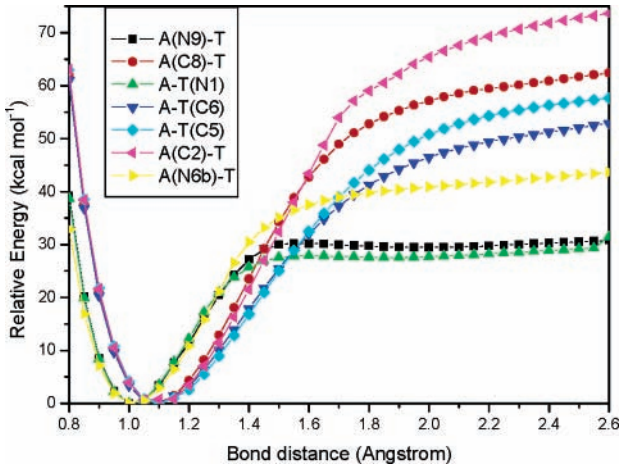

Figure 4. Potential energy surface profiles along the N−H and C−H bond dissociations in the anionic A−T base pair.

3.1. Geometries and Relative Stabilities of H-Deleted Radicals and Anions. The relative energies of optimized neutral and anionic fragments formed by stripping one hydrogen atom from the A−T pair are shown in Table 1. For the A−T base pair (Figure 1), the hydrogen abstraction and electron attachment to its fragment may result in nine neutral radicals and anions, respectively.

As shown in Table 1, predicted relative energies of the radicals spread over a range of 31.5 kcal mol^{-1}. The most stable dehydrogenated A−T base pair radical is the structure **A−T-(C5)**. The next stable species are **A(N9)−T** and **A−T(N1)**, and they are less stable than **A−T(C5)** by 9.1 and 8.0 kcal mol^{-1}, respectively. The relatively high stability can be ascribed to conjugation interactions between the resulting methylene and thymine ring in **A−T(C5)**. Furthermore, the hydrogen bonds in the A−T base pair are almost unchanged with the hydrogen loss at T(C5) as shown in Figure 3.

TABLE 1: Relative Energies (RE in kcal Mol^{-1}) of the Dehydrogenated Neutral and Anionic Radicals Derived from A−T Base Pair

	RE	
structure	radicals	anions
A(N9)−T	9.1	0.0[a]
A(C8)−T	27.8	42.7
A−T(N1)	8.0	4.8
A−T(C6)	24.0	34.7
A−T(N3)	31.5	13.1
A−T(C5)	0.0	46.1
A(C2)−T	21.9	50.9
A(N6a)−T	20.6	22.0
A(N6b)−T	16.6	18.4

[a] The energy difference ($E_{radical} - E_{anion}$) between the dehydrogenated anion [**A(N9)−T**]$^-$ and the neutral radical [**A−T(C5)•**] is 71.5 kcal mol^{-1}.

The highest-energy structure among the H-deleted radicals in Table 1 is **A−T(N3)**. As Figure 3 displays, the loss of hydrogen at T(N3) destroys the strong (N1)···H−(N3) hydrogen bond to yield **A−T(N3)**. It is noted that the distance of [A]-(C2)−H···O−(C2)[T] bond lessens from 2.836 to 2.087 Å And forms a weak hydrogen bond in the **A−T(N3)** radical.

The **A(N6a)−T** radical is generated through homolytic cleavage of the (N6a)−H bond in adenine. Removing this hydrogen atom from the NH_2 group of adenine leads to loss of the strong (N6a)−H···(O4) hydrogen bond (see Figures 1 and 2). The surviving hydrogen bond (N1)···H−(N3) gets weak with the bond length increase from 1.797 to 2.057 Å. Elimination of the hydrogen atom at other sites such as A(C2, C8, N6, N9) or T(C6, N1) may not change the hydrogen bond and conjugation interactions in the parent A−T base pair, and geometries of the dehydrogenated radicals are less changed with respect to the A−T base pair.

As Table 1 displays, for the anionic species, there are larger energy differences with respect to the neutral radicals, suggesting that the electron attachment to the A−T base pair has a significant effect on the dehydrogenation activity. In contrast to the neutral radicals, the lowest-energy dehydrogenated A−T base pair anion is the structure [**A(N9)−T**]$^-$, where the hydrogen abstraction is from the N9 site in the adenine moiety. The relatively high activity of the N9 site has been suggested in previous experimental and theoretical studies.[36−38,50−51,75]

In contrast to the neutral radicals, remarkable structural changes occur in the structures **A(N6a)−T** and **A−T(N3)** upon anion formation. The dehydrogenated anion [**A(N6a)−T**]$^-$ is higher in energy than [**A(N9)−T**]$^-$ by 22.0 kcal mol^{-1}. In the geometry optimization of [**A(N6a)−T**]$^-$, the optimized **A-(N6a)−T** radical was served as the initial structure, and the (N3)-bonded hydrogen atom in the thymine element is transferred to the N1 site in adenine, yielding the twisting species [**A(N6a)−T**]$^-$ (see Figures 1 and 2). The dehydrogenated anion [**A−T(N3)**]$^-$ is less stable than[**A(N9)−T**]$^-$ by 13.1 kcal mol^{-1}, and it has different hydrogen bond pattern from the **A−T(N3)** radical (see Figures 1 and 3). For other dehydrogenated A−T base pair radicals and anions, they have similar planar structures, although the hydrogen migration between both constituents takes place in the formation of dehydrogenated anions [**A(N9)−T**]$^-$, [**A(N6b)−T**]$^-$, and [**A(*C*2)−T**]$^-$, as shown in Figure 2.

Table 1 presents the relative stabilities of dehydrogenated A−T species. For the neutral radicals from hydrogen loss of the adenine moiety, the dehydrogenation feasibility in energy for different sites is (N9) > (N6b) > (N6a) > (*C*2) > (C8). This is in agreement with the single adenine base.[38] However,

TABLE 2: Charge Populations Concentrated at Subunits of A−T Base Pair and Charge Increments (Δq) in Their Anionic Forms by NPA

	Radicals		Anions		Δq	
structure	A	T	A	T	A	T
A(N9)−T	0.010	−0.010	−0.610	−0.390	0.620	0.380
A(C8)−T	0.033	−0.033	−0.876	−0.124	0.909	0.091
A−T(N1)	0.045	−0.045	−0.055	−0.945	0.100	0.900
A−T(C6)	0.044	−0.044	−0.051	−0.949	0.095	0.905
A−T(N3)	0.353	−0.353	−0.063	−0.937	0.416	0.584
A−T(C5)	0.041	−0.041	−0.037	−0.963	0.078	0.922
A(C2)−T	0.012	−0.012	−0.580	−0.420	0.592	0.408
A(N6a)−T	0.026	−0.026	−0.563	−0.437	0.589	0.411
A(N6b)−T	0.037	−0.037	−0.567	−0.433	0.604	0.396

TABLE 3: Adiabatic Electron Affinities (AEA), Vertical Electron Affinities (VEA), and Vertical Detachment Energies (VDE in eV) of the Dehydrogenated Radicals in the Gas Phase and in Water

	gas phase			water		
structure	AEA	VEA	VDE	AEA	VEA	VDE
A(N9)−T	3.49	2.84	4.33	5.07	4.93	5.85
A(C8)−T	2.45	1.82	2.92	4.63	4.22	5.03
A−T(N1)	3.24	2.95	3.51	5.17	4.97	5.39
A−T(C6)	2.63	2.00	3.27	4.50	4.03	4.97
A−T(N3)	3.90	2.28	4.12	5.98	4.36	5.83
A−T(C5)	1.10	0.82	1.25	2.87	2.73	2.95
A(C2)−T	1.84	0.27	3.43	3.94	2.95	5.14
A(N6a)−T	3.04	2.52	4.01	4.85	4.58	5.54
A(N6b)−T	3.02	2.43	3.95	4.79	4.59	5.49

for the neutral A−T radicals from hydrogen loss of the thymine moiety, the dehydrogenation activity is (C5) > (N1) > (C6) > (N3), differing from the isolated thymine-dehydrogenated radicals.[37]

For the dehydrogenated A−T anions from the adenine dehydrogenation, the relative stability for hydrogen-deleted pair anions at different sites is [**A(N9)−T**]$^-$ > [**A(N6b)−T**]$^-$ > [**A(N6a)−T**]$^-$ > [**A(C8)−T**]$^-$ > [**A(*C*2)−T**]$^-$, which differs from the isolated adenine-dehydrogenated radicals and anions.[38] When the dehydrogenation occurs in the thymine moiety, the resultant A−T anions characterized by their dehydrogenating sites have relative stabilities as follows: [**A(N1)−T**]$^-$ > [**A(N3)−T**]$^-$ > [**A(C6)−T**]$^-$ > [**A(C5)−T**]$^-$, different from corresponding dehydrogenated radicals and consistent with isolated thymine-dehydrogenated anions.[37] Accordingly, the formation of base pair may have a notable influence on the dehydrogenation and stability with respect to the base monomer.

3.2. Natural Population Analysis. The natural population analysis (NPA) charges in Table 2 displays the charge distribution concentrated at the components A and T in the neutral and anionic A−T base pair. To have an insight into the excess charge population, the charge increments for the structural elements in the dehydrogenated anions with respect to their neutral species are presented in Table 2. For the neutral radicals, the charge populations are quite similar, where the subunit **A** behaves as a weak donor and the **T** behaves a weak acceptor. Such positively charged populations of A in the base pair derivatives are in agreement with its relative small AEA value.[52,76−77] In comparison with **T,** the relatively notable charge transfer from **A** to **T** occurs in the **A−T(N3)** structure with an electron-transfer amount of 0.353.

It is interesting to know the excess charge populations in the dehydrogenated anions. As Table 2 shows, the H-deleted moiety generally has the dominant negative charge populations, especially for the species [**A(C8)−T**]$^-$, [**A−T(N1)**]$^-$, [**A−T(C6)**]$^-$, and [**A−T(C5)**]$^-$. The electron attachment results in the charge increments in a range from 0.078 to 0.922 for both structural subunits.

TABLE 4: Selected Thermodynamic Values for Different Dehydrogenation Channels in the Gas Phase and in Water: (A−T)$^-$ → (A−T−H)$^-$ + H (in kcal mol^{-1})

	gas phase			water		
(A−T−H)$^-$	ΔE	ΔH	ΔG	ΔE	ΔH	ΔG
A(N9)−T	18.5	19.7	13.4	−3.7	−3.1	−7.8
A(C8)−T	54.4	55.9	49.1	20.2	20.8	16.7
A−T(N1)	22.5	23.8	17.2	−5.1	−4.6	−9.6
A−T(C6)	47.7	48.9	42.4	20.4	20.8	17.0
A−T(N3)	29.6	31.0	23.4	−3.4	−2.9	−7.9
A−T(C5)	57.3	58.6	52.0	29.6	30.0	25.0
A(C2)−T	61.3	62.8	55.4	25.2	25.7	21.7
A(N6a)−T	37.0	38.5	29.9	3.8	−4.2	−0.2
A(N6b)−T	34.0	35.3	28.5	4.3	5.0	−0.6

TABLE 5: Dissociation Energies (in kcal mol^{-1}) of the Dehydrogenated A−T Radicals and Anions into Their Base Components[a]

structure	radicals	anions
A(N9)−T	14.7(13.3)	14.8(12.9)
A(C8)−T	13.3(11.8)	8.8(7.3)
A−T(N1)	12.2(10.7)	19.8(18.0)
A−T(C6)	13.4(11.5)	20.9(19.5)
A−T(N3)	13.5(11.5)	24.0(23.0)
A−T(C5)	12.2(10.8)	18.6(17.2)
A(C2)−T	11.6(10.3)	26.0(24.3)
A(N6a)−T	6.9(5.8)	11.7(10.0)
A(N6b)−T	9.8(8.5)	14.8(13.0)

[a] BSSE-corrected values in parentheses.

3.3. Electron Affinities and Energetics. The adiabatic electron affinity (AEA) for the dehydrogenated radical of the A−T base pair is an important factor for the N−H or C−H bond selective scission. As Table 3 displays, the AEA values exhibit a substantial increase as compared with corresponding single bases A (−0.28 eV) and T (0.20 eV)[78] as well as the A−T base pair (0.36 eV).[46] Since adenine has much smaller AEA value than thymine, the excess electron was expected to locate primarily in the thymine moiety for the anionic A−T base pair.[76−77] The **A−T(N3)** radical has the largest AEA value of 3.90 eV. Such high electron affinities may facilitate the loss of hydrogen atom.

The vertical electron affinity (VEA) approximately measures the necessary energy in a fast electron capture step. The dehydrogenated A−T radicals with relatively large VEA values with respect to the single base show that they are good electron captors. The **A−T(N1)** radical has the largest VEA value of 2.95 eV, while the **A(C2)−T** radical has the smallest VEA value of 0.27 eV.

To evaluate stability of the H-eliminated A−T base pair anion, the vertical detachment energy (VDE) is also estimated, and the predicted VDEs are incorporated into Table 3. The VDE values of dehydrogenated A−T base pairs vary from 1.25 to 4.33 eV, higher than that of the single base.[79] Presumably, the dehydrogenated anionic A−T base pairs have enough time to be involved in related chemical processes once they are formed.

The CPCM results in Table 3 reveal that the presence of water may stabilize dehydrogenated A−T radicals and result in remarkable increase of AEA, VEA, and VDE values in comparison with those in the gas phase. As Table 3 shows, relative magnitudes of electron affinities and detachment energies are less changed in the gas phase and in water. For example, the **A−T(N3)** radical has the largest AEA value in the gas phase (3.90 eV) and in water (5.98 eV).

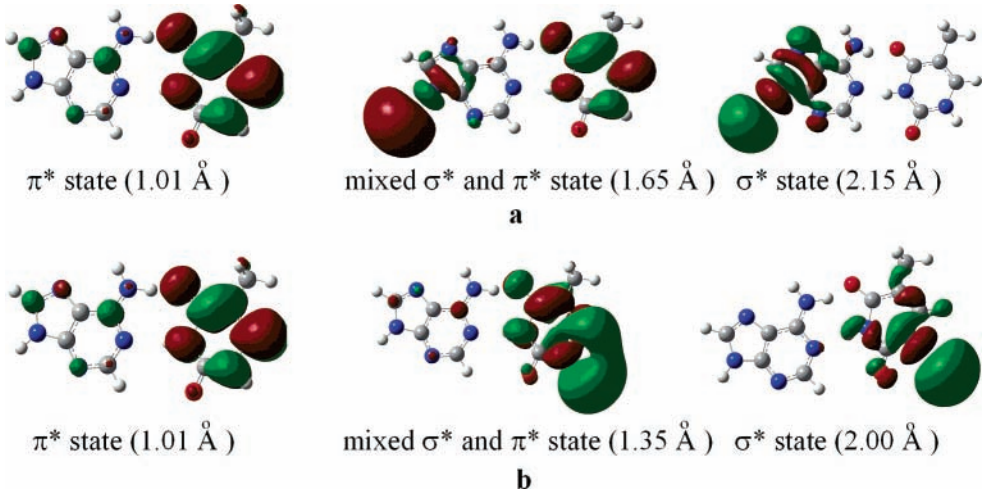

Figure 5. Evolution of singly occupied molecular orbitals in the A−T base pair anion with increase of the N9-H (a) or the N1-H (b) bond length.

Thermodynamic values for different H-deleted channels are presented in Table 4 to have more accurate description of the dehydrogenating feature of the A−T base pair. As Table 4 shows, in the gas phase, the N9-H bond dissociation in the adenine moiety is the lowest-cost process for the anionic A−T base pair with the Gibbs free energies of reaction $\Delta G°$ of 13.4 kcal mol^{-1}. The next energy-favored channel is loss of hydrogen atom at the N1 site with the Gibbs free energies of reaction $\Delta G°$ of 17.2 kcal mol^{-1}. In water, the Gibbs free energies of $\Delta G°$ for the N9-H, N1-H, and N3-H bond dissociations in the adenine moiety are −7.8, −9.6, and −7.9 kcal mol^{-1}, respectively. These CPCM results indicate that there is significant effect of the solvent water on dehydrogenation of the A−T anion.

3.4. Dissociation Energies. The dissociation energies (DE) are defined as the energy difference between the energy summation of two individually optimized bases and the fully optimized base pair. Dehydrogenation and electron attachment to the A−T base pair may modify its dissociation properties. Table 5 presents calculated dissociation energies with the BSSE correction.

The B3LYP/DZP++ calculations yield dissociation energies of 12.5 kcal mol^{-1} for the neutral A−T base pair and 16.1 kcal mol^{-1} for the anionic A−T base pair without the BSSE correction.[46] The former is in good agreement with the previous calculated result of 12.4 kcal mol^{-1} [80] and experimental value of 13.0 kcal mol^{-1}.[81] For the H-deleted A−T radicals, the **A-(N9)−T** structure has the largest dissociation energies of 13.3 kcal mol^{-1}, and the association of A(N6a) with T is relatively weak with the dissociation energy of 5.8 kcal mol^{-1}. It is noted that the **A−T(N3)** radical has dissociation energies of 11.5 kcal mol^{-1}, which is comparable to that of the neutral A−T base pair, although the strong hydrogen bond loses in **A−T(N3)**. The optimized geometry of the **A−T(N3)** radical exhibits a weak hydrogen bond [A](C2)−H···(O2)[T] (Figure 3), which can complement loss of the strong hydrogen bond [A](N1)···H−(N3)[T] to a certain extent.

For the dehydrogenated A−T anions, the dissociation energies exhibit remarkable differences as compared with the corresponding radicals except for the **A(N9)−T** structure. The dissociation of **[A(*C*2)−T]**$^-$ requires relatively large energies of 24.3 kcal mol^{-1}, while the least-cost dissociation of **[A(C8)−T]**$^-$ is endothermic by 7.3 kcal mol^{-1}.

3.5. Fragmentation Potential Energy Curve and Electronic Structure. The N−H and C−H bond scissions in the anionic A−T base pair may be described by corresponding potential energy surfaces (PES) along different dissociation channels. Figure 4 displays the PES profiles for selected N−H and C−H dissociations in the A−T anions.

As Figure 4 displays, the lower-cost dehydrogenation channels in the gas phase to **[A−T(N1)]**$^-$ and **[A(N9)−T]**$^-$ have barriers of about 27.9 and 30.2 kcal mol^{-1}, respectively. With the (N9)−H and (N1)−H bond stretching, the PES profiles rise sharply at first and then reach their maxima at about 1.45 Å. Followed by a region of plateau minimum (∼1.90 Å), the PES become relatively flat in the larger distance. For other C−H and N−H bond dissociations in A−T anion, the PES profiles apparently exhibit a monotonically increasing along the bond stretches.

Electronic structure analyses reveal that the electronic configuration of the A−T base pair anion could change during the bond dissociation. Figure 5 displays the related molecular orbital evolution at the representative (N9)−H (in adenine) and (N1)−H (in thymine) distances in the A−T anion. As Figure 5 indicates, at the equilibrium geometry ($R_{(N9)-H}$ = 1.01 Å) of the A−T anion, the excess electron occupies a low-energy π^* orbital localized in the thymine moiety. Thus, the anion can be viewed as a π^* state. As the (N9)−H bond stretches to about 1.65 Å, the electronic configuration has the mixed character of π^* and σ^* localized in the thymine and adenine moieties, respectively. At the (N9)−H bond length of ∼2.15 Å, the electronic configuration has the dominant character of σ^* localized in the adenine subunit. Therefore, the electronic structure transition should take place with dissociation of the (N9)−H bond in the adenine moiety of the base pair anion.

Similarly, in the (N1)−H bond scission of the A−T pair anion, the electronic configuration gradually varies from the π^* to the mixed $\sigma^*-\pi^*$ state localized in the thymine moiety at the (N1)−H bond separation of 1.35 Å. As the N1−H bond stretches to about 2.00 Å, the A−T base pair fragment has a character of σ^* localized in the thymine moiety. These electronic structural features for hydrogen elimination have been noticed in previous studies on single DNA bases adenine[38] and thymine.[36]

4. Concluding Remarks

The B3LYP/DZP++ method has been employed to investigate structures and relative energies of the dehydrogenated A−T base pair radicals and anions. The calculations show that the A−T base pair and its derivatives exhibit relatively high stabilities compared with the single base components. The excess

charges may modify hydrogen bond interactions and result in striking structural changes of these base pair species.

The AEA values of dehydrogenated A−T radicals range from 1.10 to 3.49 eV in the gas phase, significantly larger than those of corresponding single base constituents and the base pair. Dissociation energies of the dehydrogenated A−T species are determined in the range from 5.8 to 13.3 kcal mol^{-1} for the radicals and from 7.3 to 24.3 kcal mol^{-1} for the anions in the gas phase.

Possible N−H and C−H bond dissociations of the A−T base pair anion have been explored theoretically. The hydrogen eliminations from the (N9)−H and (N1)−H bonds are favored thermodynamically. In both dehydrogenation processes, the electronic configuration of the A−T pair fragment will gradually evolve from the π^* into σ^* state. Present results show that the A−T base pair species exhibit different electron capture effects and dehydrogenation properties from the single base, which are useful for description of the DNA strand breaking mechanism at the atomic level.

The CPCM model calculations show that there is a remarkable solvent effect on the electron attachment and dehydrogenation features of the dehydrogenated A−T radicals. The presence of water will stabilize the dehydrogenated A−T anions strikingly and facilitate dehydrogenation process of the A−T pair anion. Present results provide a basis for understanding the effect of base association on DNA breakage induced by low-energy electron attachment.

Acknowledgment. We acknowledge financial support from the National Natural Science Foundation of China (Project Nos. 20673087, 20473062, and 20423002) and the Ministry of Science and Technology (Project No. 2004CB719902).

References and Notes

(1) Demple, B.; Harrison, L. *Annu. Rev. Biochem*. **1994**, *63*, 915.
(2) Loft, S.; Poulsen, H. E. *J. Mol. Med*. **1996**, *74*, 297.
(3) Nakabeppu, Y.; Sakumi, K.; Sakamoto, K.; Tsuchimoto, D.; Tsuzuki, T.; Nakatsu, Y. *Biol. Chem.* **2006**, *387*, 373.
(4) Limoli, C. L.; Kaplan, M. I.; Phillips, J. W.; Adair, G. M.; Morgan, W. F. *Cancer Res.* **1997**, *57*, 4048.
(5) Palmer, C. M.; Serafini, D. M.; Schellhorn, H. E. *Photochem. Photobiol.* **1997**, *65*, 543.
(6) Swiderek, P. *Angew. Chem., Int. Ed*. **2006**, *45*, 4056.
(7) Cloutier, J. F.; Weinfeld, M.; O'Connor, T. R.; Castonguay, A. *J. Mol. Biol*. **2001**, *313*, 539.
(8) Lett, J. T.; Sinclair, W. K. *Advances in Radiation Biology*; Academic Press: New York, 1993.
(9) Lesczycyski, J. *Theoretical and Computational Chemistry*; Elsevier Science: Amsterdam, 1999; Vol. 8, pp 245−277.
(10) Sonntag, C. V. *Free-Radical-Induced DNA Damage and Its Repair: A Chemical Perspective*; Springer: Berlin, 2006.
(11) Sabin, J. R.; Brandas, E. *Advances in Quantum Chemistry*; Elsevier: Amsterdam, 2007; p 52.
(12) Boudaiffa, B.; Cloutier, P.; Hunting, D.; Huels, M. A.; Sanche, L. *Science* **2000**, *287*, 1658.
(13) Simons, J. *Acc. Chem. Res.* **2006**, *39*, 772.
(14) Zheng, Y.; Cloutier, P.; Hunting, D. J.; Sanche, L.; Wagner, J. R. *J. Am. Chem. Soc*. **2005**, *127*, 16592.
(15) Kundu, L. M.; Linne, U.; Marahiel, M.; Carell, T. *Chem. Eur. J*. **2004**, *10*, 5697.
(16) Giese, B.; Carl, B.; Carl, T.; Carell, T.; Behrens, C.; Hennecke. U.; Schiemann, O.; Feresin, E. *Angew. Chem., Int. Ed.* **2004**, 43, 1848.
(17) Butenandt, J.; Burgdorf, L. T.; Carell, T. *Angew. Chem., Int. Ed.* **1999**, *38*, 708.
(18) Dabkowska, I.; Rak, J.; Gutowski, M. *Eur. Phys. J. D*. **2005**, *35*, 429.
(19) Zhang, H.; Liang, Q.; Xia, Y.; Zhao, M.; Ji, Y.; Song, C.; Liu, X.; Zhang, B. *Int. J. Quantum. Chem*. **2007**, *107*, 240.
(20) Steenken, S. *Chem. Rev.* **1989**, *89*, 503.
(21) Aflatooni, K.; Gallup, G. A.; Burrow, P. D. *J. Phys. Chem. A* **1998**, *102*, 6205.
(22) Huels, M.; Hahndorf, I.; Illenberger, E.; Sanche, L. *J. Chem. Phys.* **1998**, *108*, 1309.
(23) Penhoat, M. H.; Huels, M.; Cloutier, P.; Sanche, L. *J. Chem. Phys*. **2001**, *114*, 5755.
(24) Hanel, G.; Gstir, B.; Denifl, S.; Probst, S. M.; Farizon, B.; Illenberger, E.; Mark, T. D. *Phys. Rev. Lett*. **2003**, *90*, 188104.
(25) Abdoul-Carime, H.; Langer, J.; Huels, M. A.; Illenberger, E. *Eur. Phys. J. D* **2005**, *35*, 399.
(26) Ptasinska, S.; Denifl, S.; Probst, M.; Illenberger, E.; Scheier, P.; Mark, T. D. *J. Chem. Phys.* **2005**, *123*, 124302.
(27) Pan, X.; Cloutier, P.; Hunting, D.; Sanche, L. *Phys. Rev. Lett*. **2003**, *90*, 208102.
(28) Huels, M. A.; Boudaiffa, B.; Cloutier, P.; Hunting, D.; Sanche, L. *J. Am. Chem. Soc.* **2003**, *125*, 4467.
(29) Berdys, J.; Anusiewicz, I.; Skurski, P.; Simons, J. *J. Am. Chem. Soc*. **2004**, *126*, 6441.
(30) Ptasinska, S.; Denifl, S.; Scheier, P.; Illenberger, E.; Mark, T. D. *Angew. Chem., Int. Ed*. **2005**, *44*, 6941.
(31) Sanche, L. *Eur. Phys. J. D* **2005**, *35*, 367.
(32) Desfrancois, C.; Abdoul-Carime, H.; Khelifa, N.; Schermann, J. P. *Phys. Rev. Lett.* **1994**, *73*, 2436.
(33) Desfrancois, C.; Abdoul-Carime, H.; Schermann, J. P. *J. Chem. Phys*. **1996**, *104*, 7792.
(34) Desfrancois, C.; Periquet, V.; Bouteiller, Y.; Schermann, J. P. *J. Phys. Chem. A* **1998**, *102*, 1274.
(35) Hanel, G.; Gstir, B.; Denifl, S.; Scheier, P.; Probst, M.; Farizon, B.; Farizon, M.; Illenberger, E.; Mark, T. D. *Phys. Rev. Lett*. **2003**, *90*, 188104.
(36) Li, X.; Sanche, L.; Sevilla, M. D. *J. Phys. Chem. B* **2004**, *108*, 5472.
(37) Li, X.; Sevilla, M. D.; Sanche, L. *J. Phys. Chem. B* **2004**, *108*, 19013.
(38) Xie, H.; Cao, Z. *Int. J. Quantum Chem*. **2007**, *107*, 1261.
(39) Ptasinska, S.; Denifl, S.; Gohlke, S.; Scheier, P.; Illenberger, E.; Mark, T. D. *Angew. Chem.* **2006**, *118*, 1926.
(40) Ptasinska, S.; Denifl, S.; Gohlke, S.; Scheier, P.; Illenberger, E.; Mark, T. D. *Angew. Chem., Int. Ed.* **2006**, *45*, 1893.
(41) Zheng, Y.; Cloutier, P.; Hunting, D. J.; Wagner, J. R.; Sanche, L. *J. Am. Chem. Soc*. **2004**, *126*, 1002.
(42) Gu, J.; Xie, Y.; Schaefer, H. F. *J. Am. Chem. Soc*. **2005**, *127*, 1053.
(43) Li, X.; Sanche, L.; Sevilla, M. D. *Radiat. Res.* **2006**, *165*, 721.
(44) Richardson, N. A.; Gu, J.; Wang, S.; Xie, Y.; Schaefer, H. F. *J. Am. Chem. Soc*. **2004**, *126*, 4404.
(45) Evangelista, F. A.; Schaefer, H. F. *J. Phys. Chem. A* **2004**, *108*, 10258.
(46) Richardson, N. A.; Wesolowski, S. S.; Schaefer, H. F. *J. Phys. Chem. B* **2003**, *107*, 848.
(47) Richardson, N. A.; Wesolowski, S. S.; Schaefer, H. F. *J. Am. Chem. Soc*. **2002**, *124*, 10163.
(48) Li, X.; Cai, Z.; Sevilla, M. D. *J. Phys. Chem. A* **2002**, *106*, 9345.
(49) Kumar, A.; Knapp-Mohammady, M.; Mishra, P. C.; Suhai, S. *J. Comput. Chem.* **2004**, *25*, 1047.
(50) Bera, P. P.; Schaefer, H. F. *Proc. Natl. Acad. Sci. U.S.A.* **2005**, *102*, 6698.
(51) Lind, M. C.; Bera, P. P.; Richardson, N. A.; Wheeler, S. E.; Schaefer, H. F. *Proc. Natl. Acad. Sci. U.S.A.* **2006**, *103*, 7554.
(52) Reynisson, J.; Steenken, S. *Phys. Chem. Chem. Phys*. **2002**, *4*, 5353.
(53) Bertran, J.; Oliva, A.; Sodupe, M. *J. Am. Chem. Soc*. **1998**, 120, 8159.
(54) Li, X.; Cai, Z.; Sevilla, M. D. *J. Phys. Chem. B* **2001**, *105*, 10115.
(55) Hutter, M.; Clark, T. *J. Am. Chem. Soc*. **1996**, *118*, 7574.
(56) Beek, A. D. *J. Chem. Phys*. **1993**, *98*, 5648.
(57) Lee, C.; Yang, W.; Parr, R. G. *Phys. Rev. B* **1988**, *37*, 785.
(58) Rienstra-Kiracofe, J. C.; Tschumper, G. S.; Schaefer, H. F.; Nandi, S.; Ellison, G. B. *Chem. Rev.* **2002**, *102*, 231.
(59) Boys, S. F.; Bernardi, F. *Mol. Phys.* **1970**, *19*, 553.
(60) van Duijneveldt, F. B.; van Duijneveldt van de Rijdt, J. G. C. M.; van Lenthe, J. H. *Chem. Rev.* **1994**, *94*, 1873.
(61) Reed, A. E.; Weinstock, R. B.; Weinhold, F. *J. Chem. Phys*. **1985**, *83*, 735.
(62) Reed, A. E.; Weinhold, F. *J. Chem. Phys.* **1985**, *83*, 1736.
(63) Reed, A. E.; Curtiss, L. A.; Weinhold, F. *Chem. Rev*. **1988**, *88*, 899.
(64) Reed, A. E.; Schleyer, P. V. R. *J. Am. Chem. Soc*. **1990**, *112*, 1434.
(65) Barone, V.; Cossi, M. *J. Phys. Chem. A* **1998**, *102*, 1995.
(66) Cossi, M.; Rega, N.; Scalmani, G.; Barone, V. *J. Comput. Chem*. **2003**, *24*, 669.
(67) Frisch, M. J.; Trucks, G. W.; Schlegel, H. B.; Scuseria, G. E.; Robb, M. A.; Cheeseman, J. R.; Montgomery, J. A., Jr.; Vreven, T.; Kudin, K. N.; Burant, J. C.; Millam, J. M.; Iyengar, S. S.; Tomasi, J.; Barone, V.; Mennucci, B.; Cossi, M.; Scalmani, G.; Rega, N.; Petersson, G. A.; Nakatsuji, H.; Hada, M.; Ehara, M.; Toyota, K.; Fukuda, R.; Hasegawa, J.; Ishida, M.; Nakajima, T.; Honda, Y.; Kitao, O.; Nakai, H.; Klene, M.; Li, X.; Knox, J. E.; Hratchian, H. P.; Cross, J. B.; Bakken, V.; Adamo, C.; Jaramillo, J.; Gomperts, R.; Stratmann, R. E.; Yazyev, O.; Austin, A. J.;

Cammi, R.; Pomelli, C.; Ochterski, J. W.; Ayala, P. Y.; Morokuma, K.; Voth, G. A.; Salvador, P.; Dannenberg, J. J.; Zakrzewski, V. G.; Dapprich, S.; Daniels, A. D.; Strain, M. C.; Farkas, O.; Malick, D. K.; Rabuck, A. D.; Raghavachari, K.; Foresman, J. B.; Ortiz, J. V.; Cui, Q.; Baboul, A. G.; Clifford, S.; Cioslowski, J.; Stefanov, B. B.; Liu, G.; Liashenko, A.; Piskorz, P.; Komaromi, I.; Martin, R. L.; Fox, D. J.; Keith, T.; Al-Laham, M. A.; Peng, C. Y.; Nanayakkara, A.; Challacombe, M.; Gill, P. M. W.; Johnson, B.; Chen, W.; Wong, M. W.; Gonzalez, C.; and Pople, J. A. *Gaussian 03*, Revision C.02; Gaussian, Inc.: Wallingford, CT, 2004.

(68) Sponer, J.; Leszczynski, J.; Hobza, P. *J. Phys. Chem.* **1996**, *100*, 1965.

(69) Sponer, J.; Hobza, P.; Schleyer, P. V. R. *Encyclopedia of Computational Chemistry*; Wiley: New York, 1998; pp 777−789.

(70) Guerra, C. F.; Bickelhaupt, F. M. *Angew. Chem., Int. Ed.* **1999**, *38*, 2942.

(71) Bertran, J.; Oliva, A.; Rodriguez-Santiago, L.; Sodupe, M. *J. Am. Chem. Soc.* **1998**, *120*, 8159.

(72) Mo, Y. *J. Mol. Modeling* **2005**.

(73) Sponer, J.; Jurecka. P; Hobza, P. *J. Am. Chem. Soc.* **2004**, *126*, 10142.

(74) Saenger, W. *Principles of Nucleic Acid Structure*; Springer-Verlag: Berlin, 1984; pp 123−124.

(75) Evangelista, F. A.; Paul, A.; Schaefer, H. F. *J. Phys. Chem. A* **2004**, *108*, 3565.

(76) Russo, N.; Toscano, M.; Grand, A. *J. Comput. Chem.* **2000**, *14*, 1243.

(77) Al-Jihad, I.; Smets, J.; Adamowicz, L. *J. Phys. Chem. A* **2000**, *104*, 2994.

(78) Wesolowski, S. S.; Leininger, M. L.; Pentchev, P. N.; Schaefer, H. F. *J. Am. Chem. Soc.* **2001**, *123*, 4023.

(79) Profeta, L. T. M.; Larkin, J. D.; Schaefer, H. F. *Mol. Phys.* **2003**, *101*, 3277.

(80) Sponer, J.; Leszczynski, J.; Hobza, P. *J. Phys. Chem.* **1996**, *100*, 1965.

(81) Yanson, I. K.; Teplitsky, A. B.; Sukhodub, L. F. *Biopolymers* **1979**, *18*, 1149.